International Journal of Modern Physics B, Vol. 15, Nos. 19 & 20 (2001) 2535–2548

INCOMMENSURATE STRUCTURE FACTOR IN A HOLE-DOPED SPIN-1 SYSTEM

INDRANI BOSE and EMILY CHATTOPADHYAY

Department of Physics, Bose Institute,
93/1, A.P.C. Road, Calcutta-700009, India

The nickelate compound Y_2BaNiO_5 is a spin-1 Haldane-gap antiferromagnet. The compound is doped with holes on replacing the off-chain Y^{3+} ions by Ca^{2+} ions. Inelastic neutron scattering (INS) experiments reveal the existence of sub-gap states on doping. A recent INS experiment provides evidence for an incommensurate double-peaked structure factor $S(q)$ corresponding to the sub-gap states. In this paper, we formulate a microscopic theory for the origin of the incommensurate peaks.

PACS number(s): 75.10 Jm, 71.27.+a

1. Introduction

Hole-doped quantum spin systems exhibit a variety of novel phenomena as a function of the dopant concentration. The cuprates, which become high-temperature superconductors on doping, are the prime examples of such systems. The cuprates have a rich T versus x phase diagram, where T is the temperature and x the dopant concentration.[1–3] In the undoped state, the compounds exhibit antiferromagnetic (AFM) long range order (LRO) below the Néel temperature T_N. The dominant electronic and magnetic properties of the cuprates are associated with the copper-oxide (CuO_2) planes. On the introduction of a few percent of holes, the AFM LRO is rapidly destroyed leaving behind a spin-disordered state. The hole-doped CuO_2 plane is an example of a quantum spin liquid (QSL) in 2D. Simpler AFM doped spin systems include the two-chain ladder compounds $LaCuO_{2.5}$[4] and $Sr_{14-x}Ca_xCu_{24}O_{41}$[5] and the spin-1, linear chain AFM compound $Y_{2-x}Ca_xBaNiO_5$.[6] These quasi-1D systems exhibit phenomena some of which are similar to those observed in the cuprate systems. For example, the doped ladder compound $Sr_{14-x}Ca_xCu_{24}O_{41}$[5,7] becomes a superconductor under high pressure ($T_c \sim 12$ K at a pressure of 3 Gpa). As in the cuprate systems, holes form bound pairs in the superconducting state.

The doped spin-1 compound $Y_{2-x}Ca_xBaNiO_5$ provides an example of a QSL in 1D. The parent compound Y_2BaNiO_5 is a charge transfer insulator containing Ni^{2+} ($S = 1$) chains. The ground state of the system is spin-disordered and the spin excitation spectrum is separated from the ground state by an energy gap, the

so-called Haldane gap.[8] The compound is doped with holes on replacing the off-chain Y^{3+} ions by Ca^{2+} ions. The holes mostly appear in oxygen orbitals along the NiO chains. No metal–insulator transition takes place but the DC-resistivity $\rho_{\rm DC}$ falls by several orders of magnitude.[6] This indicates that the holes are not fully mobile but delocalized over several lattice spacings. Inelastic neutron scattering (INS) experiments reveal the existence of new states within the Haldane gap. Several studies have been carried out so far to explain the origin of the sub-gap states.[9–14]

A very recent neutron scattering experiment provides evidence for an incommensurate double-peaked structure factor $S(q)$ for the sub-gap states.[15] The INS intensity is proportional to the structure factor. For the pure compound, $S(q)$ near the gap energy of 9 meV has a single peak at the wave vector $q = \pi$, indicative of AFM correlations. For the doped compound, $S(q)$ has an incommensurate double-peaked structure factor, for energy transfer $\omega \sim 3$–7 meV, with the peaks located at $q = \pi \pm \delta q$. The shift δq is found to have a very weak dependence on the impurity concentration x for x in the range $x \in [0.04, 0.14]$. Evidence of incommensurate peaks has also been obtained in the underdoped metallic cuprates.[1] The peaks are four in number and occur at $(\pi \pm \delta q, \pi)$ and $(\pi, \pi \pm \delta q\ )$. The crucial difference from the nickelate compound is that δq is proportional to the dopant concentration x. The incommensurability has been ascribed to inhomogeneous spin and charge ordering in the form of stripes. Recently, Malvezzi and Dagotto[16] have provided an explanation for the origin of spin incommensurability in the hole-doped $S = 1$ nickelate compound. They have studied a two-orbital model using the Density Matrix Renormalization Group (DMRG) method. They have shown that a mobile hole generates AFM correlations between the spins located on both sides of the hole and this is responsible for the spin incommensurability seen in experiments. Xu *et al.*[15] have given a different explanation for the origin of incommensurability. The holes doped into the QSL ground state of the $S = 1$ chain are located on the oxygen orbitals and carry spin. They induce an effective ferromagnetic (FM) interaction between the Ni spins on both sides. The incommensurate peaks arise because of the spin density modulations developed around the holes with the size of the droplets controlled by the correlation length of the QSL. In this paper, we provide a microscopic theory of the origin of spin incommensuration in keeping with the suggestions of Xu *et al.*.

2. Microscopic Model

Various microscopic models have been proposed to explain the presence of sub-gap states.[9–14] The relevant orbitals of Ni^{2+} in the Ni-O chain are $3d_{3z^2-r^2}$ and $3d_{x^2-y^2}$.[13] An electron in the latter orbital is almost localised while the $3d_{3z^2-r^2}$ orbital has a finite overlap with the $2p_z$ orbital of the oxygen ion. In the undoped state, each Ni orbital is occupied by a single electron and the oxygen orbital is filled up. The spins on the Ni orbitals have a FM alignment, due to strong Hund's rule coupling, giving rise to total spin $S = 1$. The nearest-neighbour (NN) spins $S = 1$

interact via AFM superexchange interaction mediated through the intermediate oxygen ions. On doping, holes are predominantly introduced in the oxygen orbitals. The holes have effective spin-1/2 as each $2p_z$ orbital containing a hole is occupied by a single electron (Fig. 1).

In the undoped state, we have a chain of $S = 1$ spins. The ground state is spin-disordered and, as predicted by Haldane,[8] there is a gap in the excitation spectrum. Affleck, Kennedy, Lieb and Tasaki (AKLT)[17] have provided a physical picture for the ground state. Each spin 1 can be considered to be a symmetric combination of two spin-1/2's. Each spin-1/2 forms a singlet or valence bond (VB), $\frac{1}{\sqrt{2}}(\uparrow\downarrow - \downarrow\uparrow)$, with a NN spin-1/2. The ground state is described as a valence bond solid (VBS) in which a singlet or VB is present between each NN pair of spins. Actually, AKLT wrote down the Hamiltonian for which the VBS state is the exact ground state. The Hamiltonian is a sum over projection operators onto spin 2 for successive pairs of $S = 1$ spins and can be written as

$$H_{\mathrm{AKLT}} = J \sum_{\langle ij \rangle} \left[\mathbf{S}_i \cdot \mathbf{S}_j + \frac{1}{3} (\mathbf{S}_i \cdot \mathbf{S}_j)^2 + \frac{2}{3} \right] . \tag{1}$$

Since, in the VBS state, a singlet exists between two NN spin-1/2's, the total spin of two NN spin-1's can never be 2. Thus, the projection operator onto spin 2 acting on a NN pair of spins in the VBS state gives zero. The VBS state is the exact ground state of H_{AKLT} with eigenvalue zero. The VBS state also provides the correct physical picture for the ground state of the $S = 1$ chain interacting via the usual AFM Heisenberg Hamiltonian

$$H = J \sum_{i=1}^{N} \mathbf{S}_i \cdot \mathbf{S}_{i+1} . \tag{2}$$

This has been verified in a number of experiments.

Excitations from the VBS state are triplets (a VB is replaced by a triplet) which propagate along the chain.[18] The triplet excitation spectrum is separated from the VBS state by the Haldane gap, of the order of J. The triplet excitation spectrum has been observed experimentally in Y_2BaNiO_5. The excitation differs from a spin wave in that it propagates in a spin background with no conventional

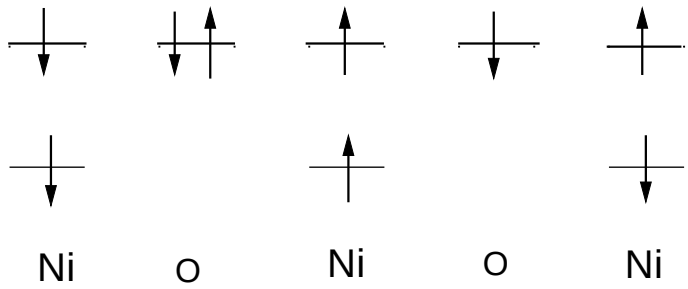

Fig. 1. Schematic diagram of the Ni-O chain with the second O being occupied by a single hole.

magnetic order. The Haldane gap Δ has a magnitude $\Delta \simeq 9$ meV.[15] The VBS state is not, however, a simple paramagnet but has quantum coherence in the form of a long-range string order.[19] On doping the nickelate compound with holes, the triplet excitation spectrum has a dispersion relation similar to that in the pure Y_2BaNiO_5. In addition, however, new states appear in the Haldane gap. Near 3 to 7 meV, the magnetic scattering is found to be the most intense along two vertical lines, displaced symmetrically from π.

The oxygen hole acts as a spin-1/2 impurity and also modifies the strength of the superexchange interaction between neighbouring Ni spins. Sørensen and Affleck[10] have considered $S = 1$ spin chains with site/bond impurities to explain the origin of sub-gap states. The holes are, however, not localized but mobile over several lattice spacings. Various models of fully mobile $S = 1/2$ holes interacting with $S = 1$ spins have been proposed so far.[11,13,20,21] The first such model is that of Penc and Shiba.[11] The effective Hailtonian is given by

$$H = H_0 + H_{J'} + H_{\tilde{t}} + H_{\tilde{J}}\,, \tag{3}$$

where

$$H_0 = J \sum_i \left[\mathbf{S}_i \cdot \mathbf{S}_{i+1} - \beta(\mathbf{S}_i \cdot \mathbf{S}_{i+1})^2\right]\,. \tag{4}$$

The special cases $\beta = 0$ and $\beta = -\frac{1}{3}$ correspond to the Heisenberg and AKLT Hamiltonians respectively. The Hamiltonian

$$H_{J'} = 2J' \sum_i (\mathbf{S}_i \cdot \boldsymbol{\sigma}_{i+1/2} + \mathbf{S}_{i+1} \cdot \boldsymbol{\sigma}_{i+1/2})\,, \tag{5}$$

describes the effect of $S = 1/2$ impurities (holes). An impurity at site $i+1/2$ changes the J coupling to J' between the $S = 1$ spins on both sides of the impurity in the Hamiltonian H_0 (Eq. (4)). Also, there is an interaction between the impurity spin σ and the adjacent $S = 1$ spins. $H_{\tilde{t}}$ and $H_{\tilde{J}}$ are the Hamiltonians describing the effective hopping of the holes on the O sites, i.e.

$$H_{\tilde{t}} = \tilde{t} \sum_i \hat{P}_i \tag{6}$$

and

$$H_{\tilde{J}} = 2\tilde{J} \sum_i \hat{P}_i (\mathbf{S}_i \cdot \boldsymbol{\sigma}_{i+1/2} + \boldsymbol{\sigma}_{i-1/2} \cdot \mathbf{S}_i)\,. \tag{7}$$

The operator $\hat{P}_i$ exchanges the occupations of the sites $i + 1/2$ and $i - 1/2$. If the hole is located on site $i + 1/2$, $\hat{P}_i$ shifts it to $i - 1/2$ provided that site is empty. Two $S = 1/2$ objects cannot occupy the same site as it costs a lot of energy. The same type of effective Hamiltonian has been used earlier to describe doped cuprate systems in a two-band (copper and oxygen orbitals) scenario.[22–24] In the cuprates too, the added holes go to oxygen sites and each hole has an effective spin-1/2 which interacts with the spin-1/2's of the Cu^{2+} ions on neighbouring sites. The major differences between the nickelate and cuprate compounds are: Ni^{2+} ion

carries spin 1 as opposed to the spin-1/2 of the Cu^{2+} ion and in the undoped state the latter compound has AFM LRO.

For the doped cuprate systems, Aharony *et al.*[25] have argued that the holes generate an effective FM exchange interaction between the Cu ions on neighbouring sites. Consider a pair of Cu ions and an intermediate hole. The interaction is described by a Hamiltonian of the type given in Eq. (5) except that the spins $\mathbf{S}_i$ have a magnitude 1/2. The exchange interaction strength J' is expected to be larger than the interaction strength J. The spins $\mathbf{S}_i$ and $\mathbf{S}_{i+1}$ prefer to be parallel irrespective of the sign of J'. The spin-1/2 of the hole along with the two spin-1/2's of the adjacent Cu-ions constitute a spin bubble or polaron. For the doped Y_2BaNiO_5 compound, a similar scenario holds true. The hole with a spin-1/2 provides a break in the VBS state of the $S = 1$ chain. The two Ni-ions which are NNs of the hole have unpaired spin-1/2's. In the absence of the hole, these two spin-1/2's form a singlet in the VBS state. In the presence of the hole, a spin bubble consisting of three spin-1/2's (the central spin belonging to the oxygen hole) is obtained. The bubbles are embedded in the original VBS state.

3. Structure Factor $S(q)$

The differential scattering cross-section in an INS experiment is proportional to the dynamical structure factor $S^{\alpha\alpha}(q,\omega)$, ($\alpha = x, y$ or z) given by[26]

$$S^{\alpha\alpha}(q,\omega) = \sum_{S',M'} \sum_{i,j} e^{\{iq(r_i - r_j)\}} \langle SM|S_i^\alpha|S'M'\rangle\langle S'M'|S_j^\alpha|SM\rangle \times \delta(\omega + E(S,M) - E(S',M'))\,. \tag{8}$$

We assume a 1D spin system at $T = 0$. The magnetic ions are located at the sites i and j with the associated magnetic form factors taken to be unity. The spin state $|SM\rangle$ is the ground state where S is the total spin of the state and M the z component of the total spin. The ground state energy is given by $E(S,M)$. The state $|S'M'\rangle$ is an eigenstate of the system with energy $E(S',M')$. The energy and momentum transfers in the scattering process are ω and q respectively.

For the doped Y_2BaNiO_5 compound, the spin states are the VBS states with spin bubbles nucleated around the doped holes. Let us consider the case of a single static hole. The total spin of the state is equal to the total spin of the bubble since the rest of the VBS state is a singlet. Since the bubble consists of three spin-1/2's, the possible spin states correspond to total spin $S = 3/2$ and 1/2 (two representations). The possible spin states $|SM\rangle$ are (only the bubble spin configurations are shown):

$$\left|\frac{3}{2},\frac{3}{2}\right\rangle = |\uparrow\uparrow\uparrow\rangle\,,$$

$$\left|\frac{3}{2},\frac{1}{2}\right\rangle = \frac{1}{\sqrt{3}}\,|\uparrow\downarrow\uparrow + \uparrow\uparrow\downarrow + \downarrow\uparrow\uparrow\rangle\,,$$

$$\left|\frac{3}{2},-\frac{1}{2}\right\rangle = \frac{1}{\sqrt{3}}\,|\downarrow\uparrow\downarrow + \downarrow\downarrow\uparrow + \uparrow\downarrow\downarrow\rangle\ ,$$

$$\left|\frac{3}{2},-\frac{3}{2}\right\rangle = |\downarrow\downarrow\downarrow\rangle\ , \tag{9}$$

$$\left|\frac{1}{2},\frac{1}{2}\right\rangle = \frac{1}{\sqrt{6}}\,|2\uparrow\downarrow\uparrow - \downarrow\uparrow\uparrow - \uparrow\uparrow\downarrow\rangle\ ,$$

$$\left|\frac{1}{2},-\frac{1}{2}\right\rangle = \frac{1}{\sqrt{6}}\,|2\downarrow\uparrow\downarrow - \uparrow\downarrow\downarrow - \downarrow\downarrow\uparrow\rangle\ , \tag{10}$$

$$\left|\frac{\tilde{1}}{2},\frac{1}{2}\right\rangle = \frac{1}{\sqrt{2}}\,|\uparrow\uparrow\downarrow - \downarrow\uparrow\uparrow\rangle\ ,$$

$$\left|\frac{\tilde{1}}{2},-\frac{1}{2}\right\rangle = \frac{1}{\sqrt{2}}\,|\downarrow\downarrow\uparrow - \uparrow\downarrow\downarrow\rangle\ . \tag{11}$$

The '˜'-sign in Eq. (11) indicates a different $S = 1/2$ representation. In the states shown in Eqs. (9) and (10), the first and the third spins (the Ni spin-1/2's) are in a $S = 1$ spin configuration. This spin 1 adds to the spin 1/2 of the hole giving rise to a resultant spin 3/2 or 1/2. In all these states, there is thus an effective FM interaction between the Ni spins. In the states shown in Eq. (11), the Ni spin-1/2's form a singlet and the hole spin is free.

Penc and Shiba[11] have calculated the hole excitation spectrum assuming a fully mobile hole. The trial wave function of the L-site periodic chain with one hole is given by

$$|SMk\rangle = \frac{1}{\sqrt{L}}\sum_j e^{ikj}\left|SM, j+\frac{1}{2}\right\rangle\ , \tag{12}$$

where $|SM, j+\frac{1}{2}\rangle$ denotes the state with the hole located at site $j+\frac{1}{2}$. With H_0 in Eq. (4) given by the AKLT Hamiltonian, the lowest hole eigenstate of H (Eq. (3)) is given by an appropriate linear combination of the states $|\frac{1}{2}\frac{1}{2}k\rangle$ and $|\tilde{\frac{1}{2}}\frac{1}{2}k\rangle$. An excited state is obtained from a different linear combination of the states. The full hole spectrum, in the subspace of states described by Eqs. (9)–(11), consists of one fourfold and two twofold degenerate bands. The dynamical structure factor has nonzero weight inside the Haldane gap due to scattering between the hole states. Penc and Shiba's microscopic model Hamiltonian has been rederived by Batista *et al.*[14] starting from a multiband Hamiltonian containing the relevant Ni and O orbitals. They have further estimated the magnitudes of the various parameters in the Hamiltonian on the basis of small cluster calculations.

We return to our consideration of a static hole. From Eq. (8), the selection rules for INS transitions are

$$\Delta S = 0, \pm 1, \qquad \Delta M = 0, \pm 1\,. \tag{13}$$

We consider $\alpha = z$ so that $\Delta M = 0$. The q-dependence of the INS intensity is given by

$$I_{S'M'}(q) = \left| \langle S'M' | \sum_i e^{iqr_i} S_i^z | SM \rangle \right|^2 . \tag{14}$$

$I_{S'M'}(q)$ corresponds to a scattering transition from the state $|SM\rangle$ to the state $|S'M'\rangle$ with an energy transfer of ω. The spin expectation values in Eq. (14) can be calculated in a straightforward manner using the method of matrix products.[27–30] In the undoped state, the Hamiltonian H in Eq. (3) reduces to H_0. We consider H_0 to be the AKLT Hamiltonian for which the VBS state is the exact ground state. In the matrix product representation, the VBS state is given by

$$|\psi_{\rm VBS}\rangle = {\rm Tr}(g_{-L} \otimes \cdots \otimes g_0 \otimes \cdots \otimes g_L) . \tag{15}$$

The 1D lattice consists of $2L+1$ sites and g_i denotes a 2×2 matrix at the ith site with single spin states as elements.

$$g_i = \frac{1}{\sqrt{3}} \begin{pmatrix} -|0\rangle & -\sqrt{2}\,|1\rangle \\ \sqrt{2}\,|\overline{1}\rangle & |0\rangle \end{pmatrix} \tag{16}$$

where $|1\rangle, |0\rangle, |\overline{1}\rangle$ are the spin-1 states with $S^z = +1, 0$ and -1 respectively. Expectation values in the matrix product states can be calculated most conveniently by the transfer-matrix method. We describe the major steps of the calculation in the following. Details of the theory of matrix product representations can be obtained from Refs. 27–30.

The norm of a wave function in the matrix product representation, e.g. $\langle \psi_{\rm VBS} \mid \psi_{\rm VBS} \rangle$ can be written as

$$\langle \psi_{\rm VBS} \mid \psi_{\rm VBS} \rangle = \sum_{\{n_\alpha, m_\alpha\}} g^\dagger_{n_1 n_2} g^\dagger_{n_2 n_3} \cdots g^\dagger_{n_L n_1} g_{m_1 m_2} g_{m_2 m_3} \cdots g_{m_L m_1} . \tag{17}$$

We define a 4×4 transfer matrix G at any lattice site by

$$G_{\mu_1 \mu_2} \Rightarrow G_{(n_1 m_1),(n_2 m_2)} = g^\dagger_{n_1 n_2} g_{m_1 m_2} . \tag{18}$$

The ordering of multi-indices is given by

$$\mu = 1, 2, 3, 4 \leftrightarrow (11), (12), (21), (22) . \tag{19}$$

With the choice of g given in Eq. (16), the transfer matrix G is

$$G = \frac{1}{3} \begin{pmatrix} 1 & 0 & 0 & 2 \\ 0 & -1 & 0 & 0 \\ 0 & 0 & -1 & 0 \\ 2 & 0 & 0 & 1 \end{pmatrix} . \tag{20}$$

The eigenvalues and eigenvectors of G are

$$\lambda_1 = 1, \qquad \lambda_2 = \lambda_3 = \lambda_4 = -\frac{1}{3} \tag{21}$$

$$|e_1\rangle = \frac{1}{\sqrt{2}}\begin{pmatrix}1\\0\\0\\1\end{pmatrix}, \quad |e_2\rangle = \frac{1}{\sqrt{2}}\begin{pmatrix}-1\\0\\0\\1\end{pmatrix}, \quad |e_3\rangle = \begin{pmatrix}0\\1\\0\\0\end{pmatrix}, \quad |e_4\rangle = \begin{pmatrix}0\\0\\1\\0\end{pmatrix}. \tag{22}$$

The normalisation (17) is determined by the largest eigenvalue for $L \to \infty$ (the size of the chain is $2L+1$):

$$\langle \psi_{\rm VBS} \mid \psi_{\rm VBS}\rangle \simeq \lambda_1^{2L+1} = 1\,. \tag{23}$$

Consider the ground state matrix element of a spin operator P at site r. One uses the notation

$$Z(P)_{\mu_1\mu_2} \Rightarrow Z(P)_{(n_1m_1),(n_2m_2)} = g^{\dagger}_{n_1n_2} P g_{m_1m_2}\,, \tag{24}$$

with $Z(1) = G$. We obtain

$$\langle P\rangle = \langle \psi_{\rm VBS} \mid \psi_{\rm VBS}\rangle^{-1} \langle \psi_{\rm VBS} \mid P \mid \psi_{\rm VBS}\rangle = (\operatorname{Tr} G^{2L+1})^{-1} \operatorname{Tr} Z(P) G^{2L}\,. \tag{25}$$

On taking the limit $L \to \infty$, we obtain

$$\langle P\rangle = \lambda_1^{-1} \langle e_1 | Z(P) | e_1\rangle\,. \tag{26}$$

For 2-site correlations of operators A_1 and B_r at sites 1 and r respectively, one obtains

$$\langle A_1 B_r\rangle = \operatorname{Tr}(G^{2L+1})^{-1} \operatorname{Tr} Z(A) G^{r-2} Z(B) G^{2L+1-r}\,. \tag{27}$$

For $L \to \infty$, the expectation value reduces to

$$\langle A_1 B_r\rangle = \sum_{n=1}^{4} \lambda_n^{-2} \left(\frac{\lambda_n}{\lambda_1}\right)^r \langle e_1 | Z(A) | e_n\rangle \langle e_n | Z(B) | e_1\rangle\,, \tag{28}$$

where λ_n and $|e_n\rangle$ are the eigenvalues and eigenvectors of the transfer matrix G. In the same way, one can calculate off-diagonal expectation values of the type $\langle S'M'|A_i|SM\rangle$.

The VBS state with a single embedded hole has different matrix product representations depending on the configuration of the three-spin bubble centred around the hole. The possible bubble spin configurations are given in Eqs. (9)–(11). For example, the states $|\frac{3}{2}\frac{3}{2}\rangle$ and $|\frac{1}{2}\frac{1}{2}\rangle$ are of the form

$$\operatorname{Tr}(g_{-L} \otimes \cdots \otimes g_{-1} \otimes g^h \otimes g_0 \otimes \cdots \otimes g_L) \tag{29}$$

with the hole located in between the sites -1 and 0. The corresponding matrix g^h is given by

$$g_h = \begin{pmatrix} 0 & 0 \\ -\sqrt{2}\,|\uparrow\rangle & 0 \end{pmatrix}, \tag{30}$$

for the $|\frac{3}{2}\frac{3}{2}\rangle$ state and

$$g_h = \frac{1}{\sqrt{3}} \begin{pmatrix} -|\uparrow\rangle & 0 \\ -2|\downarrow\rangle & |\uparrow\rangle \end{pmatrix} \tag{31}$$

for the $|\frac{1}{2}\frac{1}{2}\rangle$ state.

We have calculated $I_{S'M'}(q)$ in Eq. (14) by taking the ground state $|SM\rangle$ to be the $|\frac{1}{2}\frac{1}{2}\rangle$ state and the state $|S'M'\rangle$ to be a state which satisfies the selection rule $\Delta S = 0, \pm 1$ and $\Delta M = 0$. For example, the state $|S'M'\rangle$ can be any one of the states $|\frac{3}{2}\frac{1}{2}\rangle$, $|\frac{1}{2}\frac{1}{2}\rangle$ and $|\tilde{\frac{1}{2}}\frac{1}{2}\rangle$. In the first two cases, $I_{S'M'}(q)$ is calculated as (apart from numerical prefactors)

$$I_{S'M'}(q) = \left| \frac{(1+e^K)\cos(\frac{q}{2})}{\cosh K + \cos q} \right|^2 \tag{32}$$

where $K^{-1} = (1/\ln\ 3)$ is the spin correlation length in the VBS state. For the state $|\frac{3}{2}\frac{1}{2}\rangle$,

$$g_{\rm h} = \sqrt{\frac{2}{3}} \begin{pmatrix} |\uparrow\rangle & 0 \\ -|\downarrow\rangle & -|\uparrow\rangle \end{pmatrix}. \tag{33}$$

Also, i, j in Eq. (8) denote the sites at which the Ni spins are located, i.e. the hole spin is not explicitly taken into account. When $|S'M'\rangle$ is $\left|\tilde{\frac{1}{2}}\frac{1}{2}\right\rangle$,

$$g_{\rm h} = \begin{pmatrix} |\uparrow\rangle & 0 \\ 0 & |\uparrow\rangle \end{pmatrix} \tag{34}$$

and $I_{S'M'}(q)$ is given by (apart from a numerical prefactor),

$$I_{S'M'}(q) = \left| \frac{(1+e^K)\sin(\frac{q}{2})}{\cosh\ K + \cos q} \right|^2 . \tag{35}$$

Xu *et al.*[15] have suggested a form (Eq. (32)) for the structure factor of the ground state with a single FM bond inserted within an infinite chain. The FM bond occurs between the sites -1 and 0. In the matrix product representation, such a state is given by

$$|\psi_{\rm FM}\rangle = {\rm Tr}(g_{-L} \otimes \cdots \otimes g^a_{-1} \otimes g_0 \otimes \cdots \otimes g_L)\,, \tag{36}$$

where

$$g^a = \begin{pmatrix} \sqrt{2}\,|1\rangle & 0 \\ -|0\rangle & 0 \end{pmatrix}. \tag{37}$$

Calculation of $S(q)$ with $|S'M'\rangle = |SM\rangle = |\psi_{\rm FM}\rangle$ reproduces the form in Eq. (32). This, however, corresponds to elastic neutron scattering whereas the incommensurate signal arises from inelastic neutron scattering. The intensity $I_{S'M'}(q)$ (Eq. (32)) has two peaks symmetrically displaced from π. The widths and incommensurability are of the order of K. A good fit to the experimental data

has been obtained by treating K^{-1} as a parameter. For dopant concentrations $x = 0.04$, 0.095 and 0.14, the best fits to the experimental data are obtained for $K^{-1} = 8.1 \pm 0.2, 7.3 \pm 0.2$ and 7.2 ± 0.5 respectively. These values are considerably higher than the VBS value of $K^{-1} = (1/\ln 3)$ and are closer to the estimate of the correlation length for the Heisenberg Hamiltonian. The use of the AKLT Hamiltonian has, however, enabled us to formulate a microscopic theory of the structure factor, based on the matrix product representation. The double-peaked incommensurate structure is correctly reproduced in the theory. The intensity $I_{S'M'}(q)$, however, has nodes at $q = (2n+1)\pi$ which are not seen experimentally. Xu *et al.*[15] have suggested that finite hole densities as well as an explicit consideration of the hole spin distributed over l lattice sites centred on the FM bond, gives rise to a nonzero intensity at $q = (2n + 1)\pi$. Microscopic calculations along these lines are, however, yet to be carried out.

The structure factor $S(q)$ of INS is obtained on integrating the dynamical structure factor $S(q, \omega)$ in Eq. (8) over energy ω and is given by the sum over

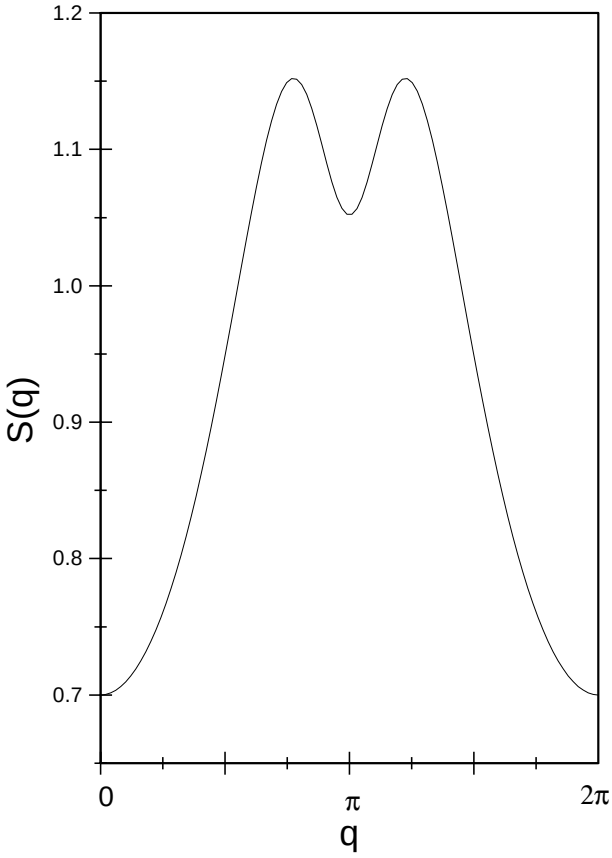

Fig. 2. Structure factor $S(q)$ versus q for $K = 1.2$.

the intensities $I_{S'M'}(q)$'s for the three possible states $|S'M'\rangle$. Two of the intensities is proportional to $\cos^2(q/2)$ while the third is proportional to $\sin^2(q/2)$. The first two intensities have a minimum at $q = \pi$ and the last intensity has a maximum at $q = \pi$. The resultant intensity for $K = \ln 3 \sim 1.1$ has a double-peaked incommensurate structure but the intensity at $q = \pi$ has a magnitude very close to that of the peak intensities. For $K = 1.2$ (correlation length less than NN Ni–Ni distance but more than the distance separating NN Ni and oxygen ions), the structure factor $S(q)$ versus q is shown in Fig. 2. The double-peaked structure is, however, very sensitive to the value of K and disappears for $K \leq 1.0$. For exchange interactions of the Heisenberg-type, K is around 0.17. With a ground state $|SM\rangle = |\frac{1}{2}\frac{1}{2}\rangle + x|\tilde{\frac{1}{2}}\frac{1}{2}\rangle (x < 1)$, the structure factor $S(q)$ contains terms proportional to $\cos^2(q/2)$ as well as $\delta \sin^2(\frac{q}{2})$ ($\delta < 1$ is a x-dependent number). With the appropriate choice of δ, a double-peaked incommensurate structure factor $S(q)$ is obtained for a wide range of values of K. Figure 3 shows $S(q)$ versus q for $\delta = 0.35$ and $K = \ln 3$. Eigenfunctions which are linear combinations of the states $|\frac{1}{2}\frac{1}{2}\rangle$ and $|\tilde{\frac{1}{2}}\frac{1}{2}\rangle$ are obtained when mobile holes are considered. In fact, as mentioned earlier, for fully mobile holes, the lowest two hole bands correspond to linear combinations

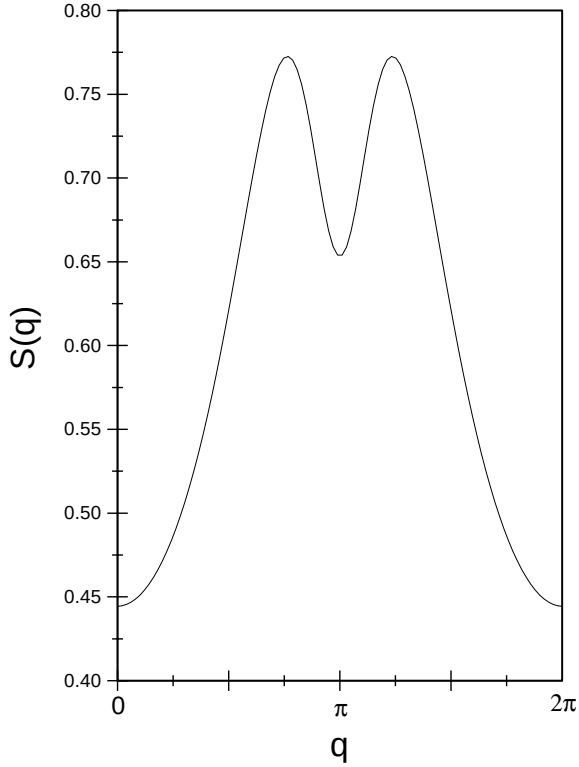

Fig. 3. Structure factor $S(q)$ versus q for $K = \ln 3$ and $\delta = 0.35$.

of the states $|\frac{1}{2}\frac{1}{2}k\rangle$ and $|\tilde{\frac{1}{2}}\frac{1}{2}k\rangle$ with $|SMk\rangle$ defined as in Eq. (18). Holes in the doped nickelate compound are not, however, fully mobile. Calculations, taking into account the limited mobility of a hole as well as an explicit consideration of the hole spin in calculating $S(q)$, are in progress and the results will be reported elsewhere.

4. Conclusion

In this paper, we have provided a microscopic theory for the double-peaked structure of the INS intensity for the doped $S = 1$ AFM compound Y_2BaNiO_5. The spin-1's are assumed to interact via the AKLT Hamiltonian for which the VBS state is known to be the exact ground state. The introduction of holes in the system nucleates spin bubbles around the holes due to the strong AFM exchange interactions between the hole spins and NN free spin-1/2's of the VBS state. The scattering between the hole states gives rise to states within the Haldane gap with an incommensurate structure factor. The incommensurate peaks occurring in the underdoped metallic cuprate systems have been ascribed to the formation of spin and charge inhomogeneities in the form of stripes. As a consequence of this, the shift δq of the location of an incommensurate peak from π is proportional to the dopant concentration x. For the doped nickelate system, δq has a very weak dependence on x for x in the range 0.04–0.14 and no experimental evidence of stripes has been obtained. Incommensuration in the doped cuprate systems occurs in the metallic state when holes are fully mobile. In the doped cuprates, the spin-spin correlations have a longer range than in the case of the doped nickelate system. This gives rise to greater effective interactions between the spin bubbles in the former case.

Malvezzi and Dagotto[16] have considered a two-orbital model for the doped Y_2BaNiO_5 compound and have shown that spin incommensurability is obtained in a wide range of densities and couplings. AFM correlations are dynamically generated across the holes to facilitate hole movement. The same type of correlations occur in the 1D Hubbard model and the 2D extended t–J model. In the two-orbital model, only the two Ni orbitals have been considered and oxygen orbitals have not been explicitly included in the Hamiltonian. The spin of the hole on the oxygen ion forms a singlet with the spin-1/2 in the adjacent Ni orbital (each of the two Ni orbitals contains an electron with spin-1/2) giving rise to an effective Zhang–Rice (ZR) doublet. This is analogous to a ZR singlet in the case of doped cuprate systems.[2] More detailed experiments are required to distinguish between the two mechanisms, suggested so far, on the origin of spin incommensuration in $Y_{2-x}Ca_xBaNiO_5$.

Several earlier studies on doped cuprate systems have explored the possibility of the binding of two spin bubbles in the antiferromagnetically interacting spin background. Zhang and Arovas[31] have considered the propagation of $S = 0$ holes in a VBS state and have found evidence for the binding of holes. The propagating $S = 0$ hole corresponds to a simultaneous hopping of a pair of electrons. The possibility for the binding of a pair of spin bubbles, centred around holes, in a VBS-type spin

background has not been explored as yet. Experimental evidence of the binding of holes in the doped nickelate compound does not exist. On the other hand, evidence for the binding of holes has been obtained in the case of a doped ladder compound.[3,5] Several numerical studies provide evidence for the binding of holes in a two-chain t–J ladder model.[3,32] The binding of two holes has been demonstrated exactly and analytically in a specially constructed t–J ladder model.[33] In the undoped case, this model, in an appropriate parameter regime, has a ground state identical to that of a $S = 1$ AFM Heisenberg spin chain.[34] The exact results on the binding of two holes hold true in a different parameter regime. The connection between doped spin-1 and ladder systems is not clearly established as yet. In summary, the experimental results on the $S = 1$ doped nickelate compound provide examples of the rich phenomena observed in other spin systems. Comparative studies of such systems are needed to highlight the common origins, if any, of some of these phenomena.

Acknowledgment

E. C. is supported by the council of Scientific and Industrial Research, India under sanction No. 9/15(186)/97-EMR-I.

References

1. J. Orenstein and A. J. Millis, *Science* **288**, 468 (2000).
2. E. Dagotto, *Rev. Mod. Phys.* **66**, 763 (1994).
3. P. W. Anderson, *The Theory of Superconductivity in the High-T_c Cuprates* (Princeton University Press, 1997).
4. Z. Hiroi and M. Takano, *Nature* **377**, 41 (1995); Z. Hiroi, *J. Sol. Stat. Chem.* **123**, 222 (1996).
5. M. Uehara, T. Nagata, J. Akimitsu, H. Takahasi, N. Mori and K. Kinoshita, *J. Phys. Soc. Jpn.* **65**, 2764 (1996).
6. J. F. Di Tusa *et al.*, *Phys. Rev. Lett.* **73**, 1857 (1994).
7. E. Dagotto, *Rep. Prog. Phys.* **62**, 1525 (1999).
8. F. D. M. Haldane, *Phys. Rev. Lett.* **50**, 1153 (1983); *Phys. Lett.* **93A**, 464 (1983).
9. Z.-Y. Lu, Z.-B. Su Sørensen, L. Yu, *Phys. Rev. Lett.* **74**, 4297 (1995).
10. E. S. Sorensen and I. Affleck, *Phys. Rev.* **B51**, 16115 (1995).
11. K. Penc and H. Shiba, *Phys. Rev.* **B52**, R715 (1995).
12. S. Fujimoto and N. Kawakami, *Phys. Rev.* **B52**, 6189 (1995).
13. E. Dagotto, J. Riera, A. Sandvik and A. Moreo, *Phys. Rev. Lett.* **76**, 1731 (1996).
14. C. D. Batista, A. A. Aligia and J. Eroles, *Europhys. Lett.* **43**, 71 (1998).
15. G. Xu *et al.*, *Science* **289**, 419 (2000).
16. A. L. Malvezzi and E. Dagotto, cond-mat/0011097.
17. I. Affleck, T. Kennedy, E. H. Lieb and H. Tasaki, *Phys. Rev. Lett.* **59**, 799 (1987); *Commun. Math. Phys.* **144**, 443 (1992).
18. G. Fáth and J. Sólyom, *J. Phys.: Condens. Matter* **5**, 8983 (1993).
19. M. den Nijs and K. Rommelse, *Phys. Rev.* **B40**, 4709 (1989).
20. B. Ammon and M. Imada, *Phys. Rev. Lett.* **85**, 1056 (2000).
21. H. Frahm and C. Sobiella, *Phys. Rev. Lett.* **83**, 5579 (1999).
22. V. J. Emery and G. Reiter, *Phys. Rev.* **B38**, 4547 (1988).

23. M. Ogata and H. Shiba, *J. Phys. Soc. of Jpn.* **57**, 3074 (1988).
24. H.-Q. Ding and W. A. Goddard III, *Phys. Rev.* **B47**, 1149 (1993).
25. A. Aharony, R. J. Birgeneau, A. Coniglio, M. A. Kastner and H. E. Stanley, *Phys. Rev. Lett.* **60**, 1330 (1988).
26. W. Marshall and S. W. Lovesey, *Theory of Thermal Neutron Scattering* (Oxford: Clarendon Press, 1971).
27. A. Klümper, A. Schadschneider and J. Zittartz, *Z. Phys.* **B87**, 281 (1992).
28. K. Totsuka and M. Suzuki, *J. Phys.: Condens. Matter* **7**, 1639 (1995).
29. H. Niggermann and J. Zittartz, *Z. Phys.* **B101**, 289 (1996).
30. A. K. Kolezhuk, *J. Phys.: Condens. Matter* **10**, 6795 (1998) and references therein.
31. S. C. Zhang and D. P. Arovas, *Phys. Rev.* **B40**, 2708 (1989).
32. E. Dagotto and T. M. Rice, *Science* **271**, 618 (1996).
33. I. Bose and S. Gayen, *Phys. Rev.* **B48**, 10653 (1993); I. Bose and Gayen, *J. Phys.: Condens. Matter* **11**, 6427 (1999).
34. Y. Xian, *Phys. Rev.* **B52**, 12485 (1995).